

Phase diagrams of half-filled 1D and 2D extended Hubbard model within COM

Adolfo Avella and Ferdinando Mancini

*Dipartimento di Fisica “E.R. Caianiello” - Università degli Studi di Salerno
 Unità di ricerca INFM di Salerno - Laboratorio Regionale INFM “SUPERMAT”
 Via S. Allende, I-84081 Baronissi (SA), Italy*

Abstract

The half-filled extended Hubbard model, in one and two dimensions, is studied by means of the 2-pole approximation within the Composite Operator Method with the aim at improving the possibilities to describe some of the experimental features observed for quasi-1D organic superconductors and Cu-O planes of cuprates. The phase diagrams (T - V and V - U) are analyzed with respect to the paramagnetic metal - paramagnetic insulator - charge ordered phase transitions. The relevant features of the diagrams (rank of the phase transitions, critical points, reentrant behavior) are discussed in detail.

Key words: Extended Hubbard Model, Composite Operator Method

1 Introduction

The extended Hubbard model [1] is the simplest Hamiltonian that takes into account non-local Coulomb interactions. Its relevance to the description of cuprate superconductors, fullerides and materials presenting charge ordered phases (rare-earth pnictides, vanadium oxides, manganites, magnetite, Bechgaard salts, ...) is widely recognized in the literature [2,3,4,5].

In this paper, we study the model, at half-filling in one and two dimensions, by means of the 2-pole approximation within the Composite Operator Method (COM) (see Ref. [6] and references therein). The latter, starting from the consideration that the original electrons lose their identity in presence of strong correlations, uses composite operators (i.e., operators built as products of the electronic ones) to describe the effective elementary excitations of the interacting system under analysis. The non-canonical algebra satisfied by the composite operators dictates constraints (i.e., Algebra Constraints [6]) that are

systematically used to fix the representation where the propagators are realized and self-consistently compute the unknown parameters appearing in the theory [6].

In the next sections, we will, first, briefly present the model and the method and, then, discuss the phase diagrams obtained by the application of the latter to the former. The rank of the transitions between homogeneous and charge ordered phases are studied together with the relation between such transitions and the paramagnetic metal-insulator one. The relevant features of the diagrams (critical points and reentrant behavior) are also analyzed in detail.

2 Hamiltonian, field equations and solution

The extended Hubbard model reads as

$$H = \sum_{\mathbf{i}} [-\mu c^\dagger(i)c(i) - 2dtc^\dagger(i)c^\alpha(i) + Un_\uparrow(i)n_\downarrow(i) + dVn(i)n^\alpha(i)] \quad (1)$$

where μ is the chemical potential, $c^\dagger(i) = (c_\uparrow^\dagger(i) c_\downarrow^\dagger(i))$ is the creation electronic operator in spinorial notation, $i = (\mathbf{i}, t)$, \mathbf{i} is a lattice vector of a d -dimensional square lattice, t is the hopping integral, U is the onsite Coulomb interaction, V is the intersite one, $n(i) = n_\uparrow(i) + n_\downarrow(i)$, $n_\sigma(i)$ is the number operator for electrons of spin σ . Hereafter, the hopping integral will be used as reference unit for all energies. We have used the notation $\phi^\alpha(\mathbf{i}, t) = \sum_{\mathbf{j}} \alpha_{\mathbf{ij}} \phi(\mathbf{j}, t)$, where ϕ can be any operator and $\alpha_{\mathbf{ij}}$ is the projector on the first $2d$ neighbor sites on the lattice. We have $\alpha(\mathbf{k}) = \mathcal{F}[\alpha_{\mathbf{ij}}] = 1/d \sum_{n=1}^d \cos(k_n)$, where \mathcal{F} is the Fourier transform.

We have chosen, as basic field, $\psi^\dagger(i) = (\xi^\dagger(i) \eta^\dagger(i))$, where $\xi(i) = n(i)c(i)$ and $\eta(i) = c(i) - \xi(i) = [1 - n(i)]c(i)$ are the Hubbard operators. They satisfy the following equations of motion

$$i\frac{\partial}{\partial t}\psi(i) = \begin{pmatrix} -\mu\xi(i) - 2d[tc^\alpha(i) + t\pi(i) - V\xi(i)n^\alpha(i)] \\ -(\mu - U)\eta(i) + 2d[t\pi(i) + V\eta(i)n^\alpha(i)] \end{pmatrix} \quad (2)$$

where $\pi(i) = \frac{1}{2}\sigma^\mu n_\mu(i)c^\alpha(i) + c(i)c^{\alpha\dagger}(i)c(i)$, $\sigma^\mu = (-1, \vec{\sigma})$, $n_\mu(i) = (n(i), \vec{n}(i))$ is the charge and spin number operator, $\vec{n}(i) = c^\dagger(i)\vec{\sigma}c(i)$ and $\vec{\sigma}$ are the Pauli matrices.

After the choice we made for the basis, we have computed, in the 2-pole approximation within COM [6], the retarded thermal Green's function $G(\mathbf{k}, \omega) =$

$\mathcal{F}\langle\mathcal{R}[\psi(i)\psi^\dagger(j)]\rangle$ (\mathcal{R} is the retarded operator)

$$G(\omega, \mathbf{k}) = \sum_{i=1}^2 \frac{\sigma^{(i)}(\mathbf{k})}{\omega - E_i(\mathbf{k}) + i\delta}. \quad (3)$$

where $E_i(\mathbf{k})$ are the eigenvalues of the energy matrix $\epsilon(\mathbf{k}) = m(\mathbf{k})I^{-1}(\mathbf{k})$, $I(\mathbf{k}) = \mathcal{F}\langle\{\psi(\mathbf{i}, t), \psi^\dagger(\mathbf{j}, t)\}\rangle$ is the normalization matrix of the basis and $m(\mathbf{k}) = \mathcal{F}\langle\{\mathbf{i}\frac{\partial}{\partial t}\psi(\mathbf{i}, t), \psi^\dagger(\mathbf{j}, t)\}\rangle$. The spectral weights $\sigma^{(i)}(\mathbf{k})$ can be computed as

$$\sigma_{ab}^{(i)}(\mathbf{k}) = \sum_{c=1}^n \Omega_{ai}(\mathbf{k})\Omega_{ic}^{-1}(\mathbf{k})I_{cb}(\mathbf{k}) \quad a, b = 1, \dots, n \quad (4)$$

where the matrix $\Omega(\mathbf{k})$ has the eigenvectors of $\epsilon(\mathbf{k})$ as columns [6]. For the sake of brevity, we do not report the complete expressions of E_i and $\sigma^{(i)}$, which can be found in Ref. [7]. The parameters appearing in the theory, and not connected to the Green's function under analysis ($\langle n(i)n^\alpha(i) \rangle$ and $\frac{1}{4}\langle n_\mu^\alpha(i)n_\mu(i) \rangle - \langle [c_\uparrow(i)c_\downarrow(i)]^\alpha c_\downarrow^\dagger(i)c_\uparrow^\dagger(i) \rangle$), will be self-consistently computed (the first) by calculating the density-density correlation function within the one-loop approximation [8] and (the second) by means of the local algebra constraint [6] $\langle \xi(i)\eta^\dagger(i) \rangle = 0$.

The set of self-consistent equations, fixing the parameters appearing in the theory, is highly non-linear. According to this, it is not strange at all that it admits two distinct solutions that, hereafter, we will call COM1 and COM2. The Composite Operator Method tries to give answers in the whole space of model and physical parameters and the presence of two solutions should be seen as a richness of the method. For the one-dimensional system we will consider only COM2 solution as with this, for the simple Hubbard model, we got excellent agreements with the Bethe Ansatz exact solution [9]. For the two-dimensional case, we will study both solutions as they will permit us to analyze two different behaviors that could be both observed experimentally.

3 Phase diagrams

3.1 One-dimensional system

COM2 solution for the one dimensional system reports a phase transition from the Mott insulating phase to a inhomogeneous charge ordered state of checkerboard type for positive values of the intersite Coulomb potential greater than some critical one. This result is consistent with many other studies [10,11,12]. The nature of this phase transition is not well understood yet and currently under intense investigation [11,12]. The phase diagram in the plane $V-U$ is shown in Fig. 1 (left panel). The phase transition is of the second order up to

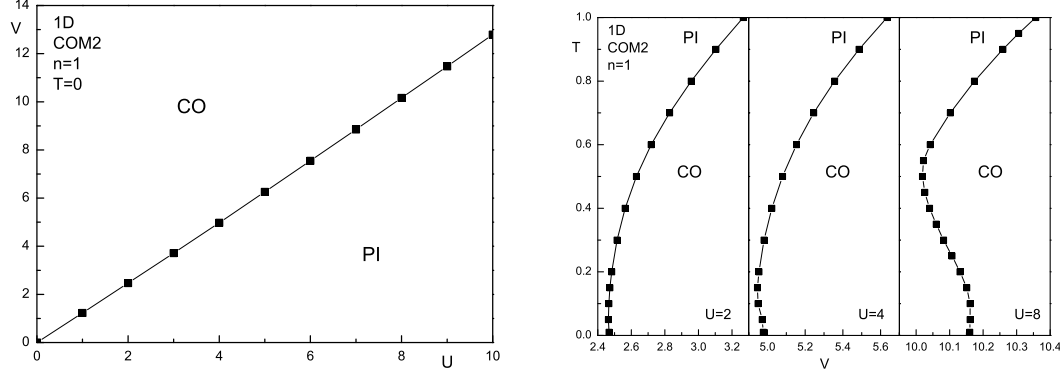


Fig. 1. (left) The phase diagram $V-U$ at zero temperature (PI = paramagnetic insulator, CO = charge ordered phase). (right) The phase diagram $T-V$ at $U = 2, 4$ and 8 .

$V \approx 2.5$; it becomes of the first order for higher values of V . The kind of phase transition that we are here analyzing is completely different from the one usually reported in the literature in proximity of the $U = 2V$ line as this latter occurs between an inhomogeneous charge ordered phase and an homogenous spin ordered phase.

In Fig. 1 (right panel) we report the phase diagram in the plane $T-V$ for $U = 2, 4$ and 8 . For $U = 2$ the transition is second order for all values of T . For $U = 4$ we can see a first signature of a reentrant behavior. By this latter we mean a situation in which by increasing the temperature we can first enter and then exit a phase when within another. For $U = 8$ the reentrant behavior is clearly evident. It is interesting to observe that the transition is continuous if there is no reentrant behavior. When instead there is a reentrant behavior, the transition is discontinuous up to the turning point, then becomes continuous. It is worth noticing that the transition is clearly marked by a discontinuity in the nearest-neighbor density-density correlation function.

3.2 Two-dimensional system: COM2

COM2 solution for the two-dimensional case has similar characteristics to that observed in the 1D case. The phase diagram in the plane $T-V$ is reported in Fig. 2. As regards the $V-U$ phase diagram, at zero temperature, we just have a transition line with slope ≈ 3 and the transition is continuous for $U \leq 1.8$ and first order for higher values of U . For finite temperature and $U = 8$ a reentrant behavior as function of temperature is clearly observed. The transition is first order up to the turning point $T = 0.6$, then becomes continuous. For $U \leq 1.8$ no reentrant behavior is observed. The fact that charge ordering may disappear by decreasing temperature has been experimentally observed in $Pr_{0.65}(Ca_{0.7}Sr_{0.3})_{0.35}MnO_3$ [13] and $La_{2-2x}Sr_{1+2x}Mn_2O_7$ ($0.47 \leq x \leq 0.62$) [14,15].

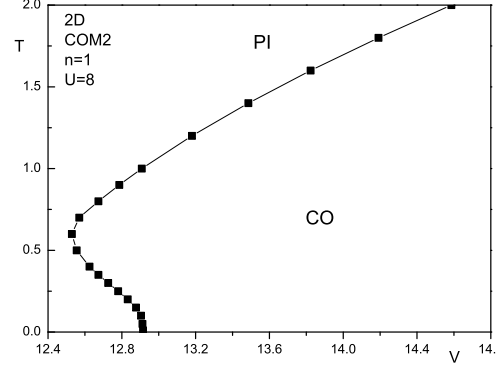


Fig. 2. The phase diagram T - V at $U = 8$.

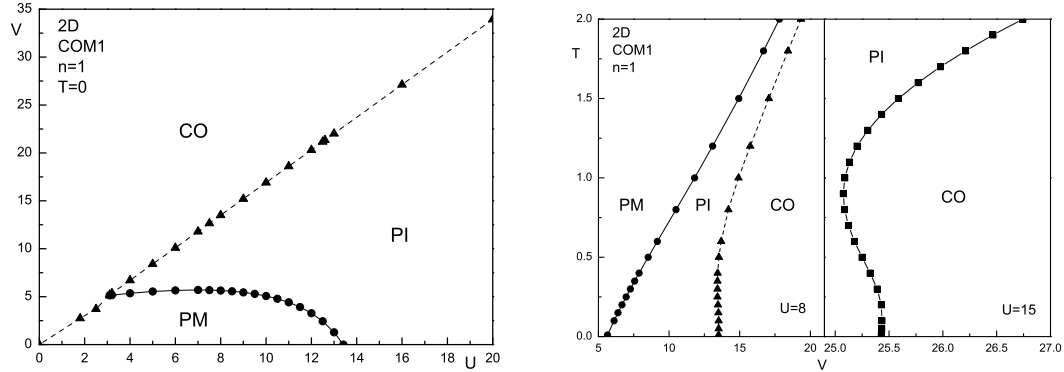


Fig. 3. (left) The phase diagram V - U at zero temperature (PM = paramagnetic metal). (right) The phase diagram T - V at $U = 8$ and 15 .

3.3 Two-dimensional system: COM1

The system undergoes a metal-insulator transition at some critical value of the onsite Coulomb potential U , which depends on the intensity of the intersite potential V . With respect to the $V = 0$ case (the simple Hubbard model), the metallic region is compressed by the presence of the intersite interaction and disappears for $V > 5.7$. By further increasing the intersite Coulomb potential, the system undergoes a transition to a charge ordered state. The complete phase diagram in the plane V - U is shown in Fig. 3 (left panel). The diagram is characterized by two critical curves, which separate the different phases. The lower one controls the MIT, the upper one controls the transition to a charge ordered state. The first transition is first order for $U \leq 12$ and second order for higher values of U ; the second one is first order for $U \geq 1.9$ and second order for lower value of U .

The phase diagram in the plane T - V is shown in Fig. 3 (right panel). For $U = 15$ there is no metallic phase and we have a critical temperature where a transition from an insulating to a charge ordered state is observed. The transition is first order up to $T = 0.95$, then becomes continuous. A reentrant

behavior is observed with the same characteristics previously discussed. For $U = 8$ we have two critical temperatures, which characterize the MIT transition and the insulator-charge order transition, respectively. Also in this case a reentrant behavior is observed in the latter transition.

4 Conclusions

The phase diagrams, in the planes $V-U$ and $T-V$, of the half-filled extended Hubbard model, in one and two dimensions, has been studied by means of the 2-pole approximation within the Composite Operator Method. Transitions between the paramagnetic (metal and insulator) phase and a charge ordered state of checkerboard type have been found. Reentrant temperature behavior in the plane $T-V$ has been observed with characteristic similar to that experimentally found for some manganites. The rank of the phase transitions has been studied and identified.

References

- [1] V. Emery, in: J. Devreese, R. Evrand, V. van Doren (Eds.) Plenum Press, New York, 1979, p. 247.
- [2] C. Varma, Sol. Stat. Comm. 62 (1987) 681.
- [3] A. Janner, Phys. Rev. B 52 (1995) 17158.
- [4] R. H. McKenzie, et al., Phys. Rev. B 64 (2001) 085109.
- [5] M. Calandra, J. Merino, R. H. McKenzie, Phys. Rev. B 66 (2002) 195102.
- [6] F. Mancini, A. Avella, Eur. Phys. J. B 36 (2003) 37.
- [7] A. Avella, F. Mancini, The hubbard model with intersite interaction within the composite operator method, to be published in Eur. Phys. J. B (2004).
- [8] F. Mancini, S. Marra, H. Matsumoto, Physica C 252 (1995) 361.
- [9] A. Avella, F. Mancini, M. Sánchez-Lopez, Eur. Phys. J. B 29 (2002) 399.
- [10] J. Hirsch, Phys. Rev. Lett. 53 (1984) 2327.
- [11] M. Nakamura, Phys. Rev. B 61 (2000) 16377.
- [12] E. Jeckelmann, Phys. Rev. Lett. 89 (2002) 236401.
- [13] Y. Tomioka, et al., J. Phys. Soc. Jpn. 66 (1997) 302.
- [14] T. Chatterji, et al., Phys. Rev. B 61 (2000) 570.
- [15] J. Dho, et al., J. Phys.: Cond. Matt. 13 (2001) 3655.